Circulation Physiology Final Report

Analysis of Solute Transport and Effects of Flow Rates on Glomerular Filtration Rate

Group 15: Hakeem Butler, Isaac Hong, Chelsea Lang, Sabrina Wueste, Justin Yun
Department of Bioengineering, University of California, Riverside, Winter 2019.

Abstract

Glomerular filtration rate represents the flow of plasma from the glomerulus into the Bowman's space per unit time and is an important indicator of kidney function. Several forces contribute to the glomerular filtration rate, including hydrostatic and oncotic pressure. Understanding the interplay of these forces in the glomerulus and Bowman's space is important for regulating filtration. Possible problems that may arise in the renal biotransport system include hypertension, kidney disease, kidney stones, blood in urine, and many more obstructions to the renal system. By understanding characteristics of glomerular blood flow, filtration, and other factors that contribute to the glomerular filtration rate (GFR), the causes for problems in kidney filtration can be determined.

COMSOL Multiphysics was used to create a steady state 2D axisymmetric model to simulate fluid flow through a porous media. The geometry consisted of rectangles that modeled the glomerulus, arterioles, and the Bowman's capsule. A stationary study is performed using steady state flow physics with free and porous media flow. This study will focus on varying the inlet flow rates and diffusivities according to different solutes to observe changes in normal total flux at the filtration boundary. GFR values will also be analyzed based on inlet and outlet flows.

I. INTRODUCTION

The kidneys function by removing wastes and extra fluid from the body, utilizing the pressure gradient created in the glomerulus to filter out water and solutes and transport blood to nephrons for further filtration and reabsorption [4]. Hypertension is common in the kidneys and occurs when blood pressure increases. It has also shown to reduce the glomerular filtration rate. Glomerular filtration rate (GFR) is an important measure of kidney function and can determine stages of chronic kidney disease. GFR is the amount of fluid filtered from the glomerulus into the Bowman's capsule over a period of time. Within the fluid, organic and inorganic solutes are freely filtered, but the glomerular filtration barrier prevents passage of certain substances based on size and charge into the Bowman's capsule. The primary forces that govern filtration in the glomerular capillaries are hydrostatic pressure and oncotic pressure. Glomerular capillary hydrostatic pressure and Bowman's space oncotic pressure favor filtration, where as Bowman's space hydrostatic pressure and glomerular capillary oncotic pressure oppose filtration [9]. The average GFR for a healthy young man is 130 ml/min, while the average GFR for a healthy young woman is 110 ml/min. A GFR below 60 ml/min is typically associated with chronic kidney disease, eventually leading to kidney failure.

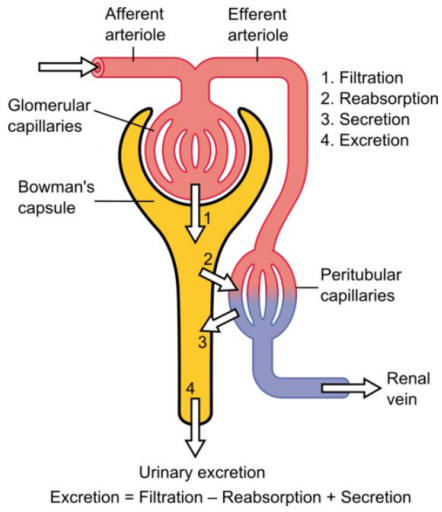

Figure 1. Basic nephron structure and function. Blood plasma and other substances get filtered from the glomerulus to the Bowman's capsule.

Previous studies have shown that changes in the afferent and efferent arteriole causes glomerular capillary hypertension. An increase in the afferent arteriolar diameter has shown to cause an increase in glomerular capillary hydrostatic pressure, causing an increase in GFR. A decrease in the afferent arteriole was shown to have an opposite effect. An increase in the diameter of the efferent arteriole causes a decrease in the glomerular capillary hydrostatic and decrease in the GFR, while a decrease in the diameter of the efferent arteriole has an opposite effect [10]. Knowing the possible GFR outcomes from pressure induced flow will contribute to the understanding of this study. This study will also build upon the past literatures in experimenting with varying inlet flow of the afferent arteriole, rather than arteriole diameter.

This report focuses on attempting to accurately represent the biological system despite the high complexity of fluid-fluid, fluid-solid, and solid-solid interactions. Endeavors for this study include analyzing the effects of solute transport on normal total flux. Solute transport includes obtaining diffusion coefficients and concentrations specific to each solute in order to simulate various filtration rates. Varying the inlet flow will also produce results that will help better understand fluid flow throughout the model. For example, reducing blood flow to the glomerulus is expected to reduce the filtration rate, causing decreased pressure in the glomerulus and limited filtrate formation.

Determining the concentration and velocity profiles of a healthy glomerulus and Bowman's capsule will allow the study to approach a better understanding on how flow in the system can be partitioned into the capillary and Bowman's capsule. The approach consists of a steady state 2D axisymmetric simulation of the glomerulus (including the afferent and efferent arteriole) and Bowman's capsule with free porous media flow for fluid mechanical analysis.

II. MODEL DESCRIPTION: OBTAINING A GEOMETRIC DEFINITION

2.1 Governing Equations

A steady state 2D model of the glomerulus and Bowman's capsule was coupled with porous media flow in COMSOL. Running the simulation produced a velocity and pressure profile in order to analyze fluid flow in the glomerulus and Bowman's capsule. The fluid being modeled is blood, therefore flow must match the density and viscosity values of real life blood flow. A density of 1060 $\frac{kg}{m^3}$ and viscosity of $3\,x\,10^{-3}\,Pa\cdot s$ were used [7]. Coupling fluid flow laws were necessary for the simulation of this slow flow into porous media model. Incompressible Navier-Stokes equation for 2D modeling was used to simulate free flow for this study [15].

$$\boldsymbol{\rho\frac{\partial\vec{v}}{\partial t}+(\rho\vec{v})\cdot\nabla\vec{v}=-\nabla p+\mu\nabla^2\vec{v}+\rho\vec{g}}$$

$$\boldsymbol{\nabla\cdot\vec{v}=0}$$

Equation 1: Incompressible Navier-Stokes Equations for Newtonian Fluid

The model also uses the Free and Porous Media Flow physics in COMSOL. The flow physics solves for Brinkman equations in porous media [17]. It is used for modeling problems where free single-phase flow is connected to porous media. Brinkman equations are derived from Darcy's Law, which describes slow flow at a distance from the channel. This physics uses the Brinkman to Navier-Stokes coupling to describe the transitions between slow flow in porous flow media and fast flow in channels described by Navier Stokes.

$$\rho\frac{\partial u}{\partial t}-\nabla\cdot\eta(\nabla u+(\nabla u)^T)-\left(\frac{\eta}{k}u+\nabla p-F\right)=0$$

Equation 2: Brinkman Equation for Free and Porous Media Flow

2.2 Biological Model

Considering normal conditions, blood flow enters the afferent arteriole from the renal artery. The blood is distributed in two areas. A portion of blood flows through the glomerular capillary beds and leaves the efferent arteriole where pressure is lower than the glomerulus. The other portion becomes filtered into the Bowman's capsule by the high pressure in the glomerulus. This interaction of the glomerulus and the Bowman's capsule within the kidney is known as the renal corpuscle. To simulate fluid mechanics of the renal corpuscle the following parameters were obtained from previous studies: blood viscosity, blood density, pressure affecting the porous media, and inlet flow velocity (Table 2). An

inlet velocity of $10.3\,mm/s$ was applied to simulate fluid flow through an average renal system [5]. This velocity value can be utilized to further find the GFR. Reference literature provided a range of GFR values from $118\,mL/min/1.73\,m^2$ to $130\,mL/min/1.73\,m^2$ [1]. To accurately represent this biological model in the computerized model, the following physics were implemented: free and porous media flow and transport of diluted species.

2.3 COMSOL Geometry

The original plan was to create a geometry (Figure 2) of the renal corpuscle with 3 rectangles that represented the glomerulus and arterioles (A), a separate porous media construct (B), and the Bowman's capsule (C). The inlet flow was set to start at the afferent arteriole and produce an outlet flow at the efferent arteriole end and the Bowman's capsule. However, meshing and flow rate problems were encountered. Therefore, a simpler model was created to see better variation in outcomes. The final geometry only consisted of two rectangles, by removing the middle porous construct. This was to help in the increase of meshing. To prevent complete fluid flow through the Bowman's capsule, the entire filtrate geometry had porous media flow physics applied to it. Also, the length of the geometry was immensely shortened in order to have fewer elements to process. This, of course, is not accurate to the literature but was necessary to have the model run in COMSOL.

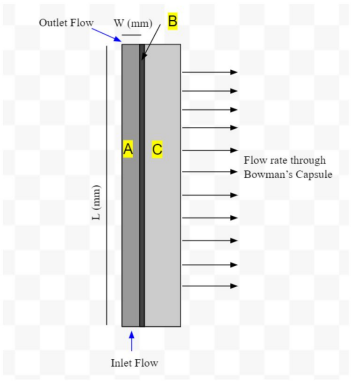

Figure 2. Original Geometry (not to scale)

Although this model is not an exact depiction of the in vivo biological anatomy, the main goal is to focus on how the flow in the system is being partitioned into the capillary and Bowman's capsule. Therefore, velocity and concentration profiles were obtained to analyze fluid dynamics within the renal corpuscle.

The complexity of the glomerulus shape was simplified by extending the tube to a linear shape, therefore the difference in geometries between the 2D model and the biological case is negligible. The geometrical lengths of glomerulus (Rectangle A) and the Bowman's capsule (Rectangle C) of the final model were not obtained from literature, but were set as arbitrary values that helped the model work more efficiently (Table 1). The width values were obtained from literature and were kept for the final model.

Table 1. Model Dimensions

Geometry	Length (*mm*)	Width (*mm*)
Rectangle A	1	$2.15\,x\,10^{-2}$ [12]
Rectangle C	1	0.2062 [8]

Table 2. Data to Parametrize the Porous Media Flow Model

Variable	Parameter	Value
$\boldsymbol{v}_{1,\text{ in}}$	Inlet Flow Rate	10.3 $\frac{mm}{s}$ [5]
$\boldsymbol{v}_{2,\text{ in}}$	Inlet Flow Rate	20.6 $\frac{mm}{s}$ [5]
$\boldsymbol{v}_{\text{out}}$	Outlet Flow Rate	8.3 $\frac{mm}{s}$
ρ	Fluid Density	1060 $\frac{kg}{m^3}$
η	Fluid Viscosity	0.003 $Pa * s$ [5]
ε	Porosity	0.1
K	Permeability	1 x 10^{-12} $\frac{m^2}{s}$
c_1	Urea Concentration	4.4 $\frac{mol}{m^3}$ [20]
D_1	Urea Diffusivity	7.6 x 10^{-10} $\frac{m^2}{s}$ [21]
c_2	Albumin Concentration	15.45 $\frac{mol}{m^3}$ [23]
D_2	Albumin Diffusivity	4.4 x 10^{-11} $\frac{m^2}{s}$ [22]
c_3	Glucose Concentration	5.5 $\frac{mol}{m^3}$ [18]
D_3	Glucose Diffusivity	6.7 x 10^{-10} $\frac{m^2}{s}$ [19]

2.4 Mesh Independence Studies

The result of the model is built by a number of high order polynomials and each element holds many degrees of freedom. This can be represented in the bigger picture as a computational domain that is composed of a mesh of elements. The resulting mesh is shown in Figure 4.

Conducting this mesh independence test of the final model required boundary probe application to the left wall of the filtrate domain. The boundary probe computed the wall shear stress using the equation fp.mu * fp.sr. The shear stress equation includes mu and sr, which represents viscosity and shear rate, respectively. By altering the mesh size, the shear stress of the wall of the filtrate domain varies. According to the results in Table 3, mesh independence failed. However, normal mesh was deemed sufficient for representing the model because it minimizes the difference between the exact and approximate solution. Because of the finite computational resources and time, the computational model must rely on an approximation of the real solution.

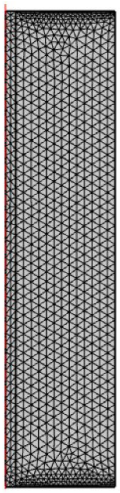

Figure 4. Applied mesh (Normal size)

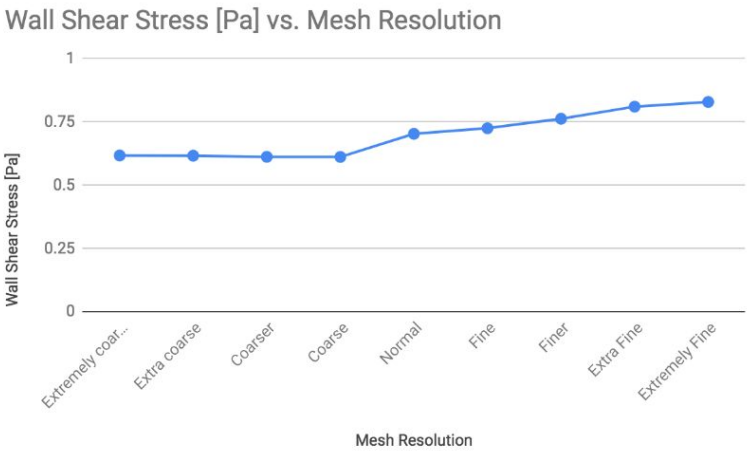

Figure 5. Mesh Independence Plot

Table 3. Mesh Independence

Mesh Resolution	Wall Shear Stress [Pa]	Percent Change
Extremely coarse	0.61762	0%
Extra coarse	0.61682	0.1295%
Coarser	0.61239	0.7182%
Coarse	0.61192	.0767%
Normal	0.70322	14.9202%
Fine	0.72543	3.1583%
Finer	0.76284	5.1569%
Extra Fine	0.81072	6.2765%
Extremely Fine	0.82927	2.2881%

2.5 Boundary Conditions

Application of flow in fluid dynamics are approximations considering that flow can become skewed. At the afferent arteriole, a spatially uniform inflow velocity profile was constructed to add different diffusivities to simulate different solutes flowing through the model. The outlet flow was designated at the efferent arteriole and the Bowman's capsule with an open boundary condition. The walls of the model are assumed to be sedentary, therefore a no-slip boundary condition was applied. Another boundary condition included was symmetry, which is very common in tube flow.

III. RESULTS

3.1 Results

For this final study, a model that represents the fluid flow and filtration through the glomerulus and filtrate domain was built using parameter values shown in Table 2. COMSOL was used to simulate a 2D steady flow observing fluid-fluid interactions. To determine how inlet velocity affects the model, a literature value of 10.3 $\frac{mm}{s}$ was used as the rate (Figure 6.1). The figure shows that the Bowman's capsule experiences zero velocity. Despite this, there are velocities present at the afferent and efferent ends of the glomerulus domain. The outlet shows negative values starting from $4.0\,x\,10^{-4}\,\frac{mm}{s}$. The negative values may be due to turbulent flow at that part of the domain. In Figure 6.2, the inlet flow was doubled to 20.6 $\frac{mm}{s}$. A similar velocity plot was obtained where significant values were only seen at the ends of the glomerulus domain. The only difference was the increase in value at the inlet region. Both of the velocities were taken into consideration for use with the transport of diluted species.

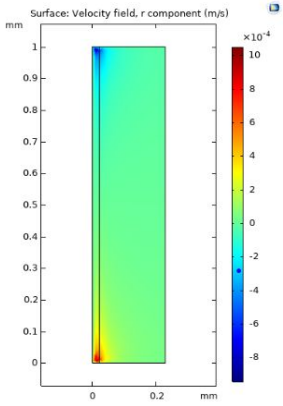

Figure 6.1 Velocity plot at Inlet flow of 10.3 mm/s

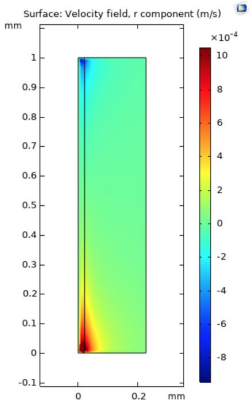

Figure 6.2 Velocity Plot at Inlet flow of 20.6 mm/s

Concentration plots were obtained; however, both velocities had the exact same results. The key assumption made with dilute species is velocity affects the concentration profile through convection, but the motion of dilute species is too small to affect the velocity field. Therefore, the initial literature value of 10.3 $\frac{mm}{s}$ was utilized. Diffusivity coefficients and concentrations were researched and used to parameterize the solutes in the model (Table 2). Glucose, urea, and albumin were chosen due to their significance in the kidney filtration system. These solutes were simulated with the transport of diluted species physics through a filtrate domain. All these solutes were considered to be in blood, therefore the blood viscosity was kept constant for all solute tests. The concentration plots are needed to observe the partitioning of each solute throughout the model.

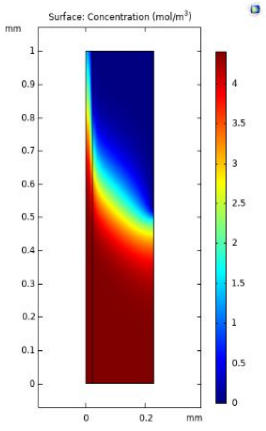

Figure 8.1 Concentration Plot of Urea solute (at 10.3 mm/s and 20.6 mm/s)

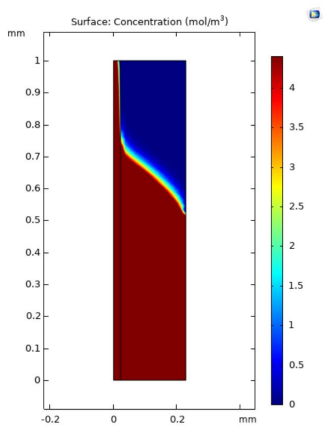

Figure 8.2 Concentration Plot of Albumin solute (at 10.3 mm/s and 20.6 mm/s)

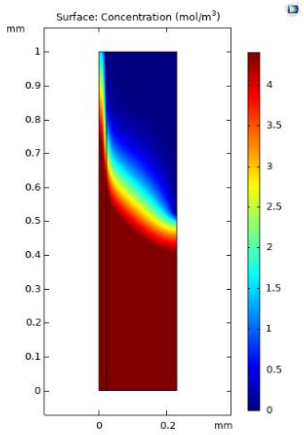

Figure 8.3 Concentration Plot of Glucose solute (at 10.3 mm/s and 20.6 mm/s)

Figure 8.1 shows that urea enters with an average concentration value of 4 $\frac{mol}{m^3}$. As it moves upwards, the solute is filtered into the Bowman's capsule due to the large concentration of urea that is observed in that domain. Eventually, the solute approaches the efferent end where the concentration decreases to 1 $\frac{mol}{m^3}$. The concentration plot for glucose (Figure 8.3), has a very similar profile as urea. This is due to the similarity in diffusivity and concentration values of these solutes in the blood. To obtain variation, albumin was tested since the molecular size of this solute is much larger than that of glucose and urea. The diffusivity coefficient is slightly smaller, but still on the same order of magnitude compared to other solutes (Table 2). Figure 8.2 represents albumin concentration profile. It is observed that there is an slight increase in high concentration of albumin in the domain, compared to other solutes. This is because albumin is stuck in the filtrate barrier due to its large size and low diffusivity. These results can be used to observe changes in total flux across the boundary of the filtrate domain.

Table 4. Boundary Probe - Normal Total Flux

Solute	Normal total flux ($\frac{mol}{s}$)
Urea (v_1)	5.5930×10^{-11}
Urea (v_2)	1.1715×10^{-10}
Albumin (v_1)	1.9084×10^{-10}
Albumin (v_2)	4.0525×10^{-10}
Glucose (v_1)	6.9175×10^{-11}
Glucose (v_2)	1.4623×10^{-10}

Table 5. Boundary Probe - Velocity Magnitude

Inlet velocity	Velocity magnitude ($\frac{m^3}{s}$) *At the inlet (afferent arteriole)*	Velocity magnitude ($\frac{m^3}{s}$) *At exit of the filtrate domain*
10.3 mm/s	1.495×10^{-11}	2.1717×10^{-11}
20.6 mm/s	2.9915×10^{-11}	3.4507×10^{-11}

A boundary probe was taken on the outer wall of the Bowman's capsule to collect the amount of solute exiting the system through the filtrate. The boundary probe computed the integral of the equation tds.ntflux_c to obtain normal total flux values across the boundary. Building off of the information from the previous profiles, the two different velocities were utilized to determine normal total flux in the case of each solute scenario. These values can be found above in Table 4. $\boldsymbol{v}_1$ represents the literature velocity of $10.3\ \frac{mm}{s}$ and $\boldsymbol{v}_2$ represents the doubled rate of $20.6\frac{mm}{s}$. There were no significant flux value differences when comparing $\boldsymbol{v}_1$ and $\boldsymbol{v}_2$ for each solute. However, it clearly shows that higher inlet flow (in this case, the doubled rate) results in a larger normal total flux. Compared to glucose and urea, albumin had a slightly smaller total flux. This is a reasonable conclusion considering how the diffusion coefficient for albumin is smaller than the other solute coefficients.

Another boundary probe was applied at the afferent arteriole and at the exit of the filtrate domain to observe the GFR. The values obtained are shown in Table 5. A lower velocity magnitude is expected at the exit of the filtrate domain and the ratio between the velocity at the afferent arteriole and exit of the filtrate domain should be used to observe GFR. However, our results are inconclusive as the velocity magnitude observed exiting the system was higher than the velocity magnitude at the inlet at the afferent arteriole.

IV. DISCUSSION

Our preliminary model analyzed the interaction between arterioles, glomerulus, porous membrane, and Bowman's capsule. Explicitly modeling our preliminary model required running an accurate number of elements. The thin membrane used as our porous media construct created a massive number of elements that exceeded computational power. To solve this, the porous construct was removed to reduce time limitations. Neglecting the thin porous membrane causes fluid to freely flow to the exit. Therefore, the Bowman's capsule was converted into a porous media domain in order to filtrate the fluid. This helps in providing the basis for a model that can take place in pressure based flow. The model was also shortened in order to decrease the number of elements. Although this is biologically inaccurate, it allowed for the computation of better results than the preliminary model.

Normally 20% of the overall blood flow represents GFR from the Bowman's capsule [24]. However the GFR results from this study showed that the outlet flow was greater than the inlet flow. This is impossible if filtration is to be accurately modeled. The issues that may have caused this could be due to the wrong application of physics and how obtaining values from separate studies may not work well together. If possible, future values should be collected from the same study. The final model can not be compared to the resulting models of the cited literature due to the discussed errors. Also, a 2D model was utilized although most literature focused on a 3D studies with volumetric values. Therefore, the obtained results are not as representative of the biological system.

The complications in creating a well-functioning model are caused by the complex structure of the glomerular capillaries. This issue can be resolved by redirecting focus to a sectional area of this system, assuming that filtration rate is relatively constant throughout the entire glomerulus. For additional future work, a pressure-driven flow would be an accurate study to represent the biological model of glomerular filtration. The pressure differences between the afferent and efferent arterioles create a pressure gradient in the glomerulus, influencing filtration. If this study is pursued, it could help with

modeling hypertension and hypotension effect on kidney filtration. Not only will pressure induced flow provide a more authentic representation of the biological process, a 3D model would match the complexity of the system.

VI. REFERENCES

[1] Pierre, Schaeffner, Elke, Ebert, Natalie, Etienne, . . . Cavalier. (2012, July 01). Normal reference values for glomerular filtration rate: What do we really know? Retrieved February 17, 2019, from https://academic.oup.com/ndt/article/27/7/2664/1850733

[2] Stevens, L. A., Coresh, J., Greene, T., & Levey, A. S. (2006). Assessing Kidney Function — Measured and Estimated Glomerular Filtration Rate. *New England Journal of Medicine,354*(23), 2473-2483. doi:10.1056/nejmra054415

[3] Deen, W. M. (2004). What determines glomerular capillary permeability? *Journal of Clinical Investigation,114*(10), 1412-1414. doi:10.1172/jci23577

[4] Cole, L., & Kramer, P. R. (2016). The Kidney Filtration System. *Human Physiology, Biochemistry and Basic Medicine,*109-110. doi:10.1016/b978-0-12-803699-0.00030-x

[5] Takenaka, T., Harrison-Bernard, L. M., Inscho, E. W., Carmines, P. K., & Navar, L. G. (1994). Autoregulation of afferent arteriolar blood flow in juxtamedullary nephrons. *American Journal of Physiology-Renal Physiology,267*(5). doi:10.1152/ajprenal.1994.267.5.f879

[6] Ferrell, N., Sandoval, R. M., Bian, A., Campos-Bilderback, S. B., Molitoris, B. A., & Fissell, W. H. (2015). Shear stress is normalized in glomerular capillaries following % nephrectomy. *American Journal of Physiology-Renal Physiology,308*(6). doi:10.1152/ajprenal.00290.2014

[7] Cutnell, J. D., & Johnson, K. W. (1998). *Physics, 308*. New York: Wiley.

[8] Sasaki, T., Tsuboi, N., Haruhara, K., Okabayashi, Y., Kanzaki, G., Koike, K., . . . Yokoo, T. (2018). Bowman Capsule Volume and Related Factors in Adults With Normal Renal Function. *Kidney International Reports, 3*(2), 314-320. doi:10.1016/j.ekir.2017.10.007

[9] Glomerular Filtration And Renal Blood Flow. (2007). *Renal Physiology,*31-46. doi:10.1016/b978-0-323-03447-0.50009-4

[10] Feher, J. (2012). Regulation of Fluid and Electrolyte Balance. *Quantitative Human Physiology,*665-673. doi:10.1016/b978-0-12-382163-8.00074-8

[11] Bohle, A., Aeikens, B., Eenboom, A., Fronholt, L., Plate, W. R., Xiao, J., . . . Wehrmann, M. (1998). Human glomerular structure under normal conditions and in isolated glomerular disease. Kidney International,54. doi:10.1046/j.1523-1755.1998.06742.x

[12] Navar, G., & Richfield, O. (2018). Faculty of 1000 evaluation for Novel hemodynamic structures in the human glomerulus. *F1000 - Post-publication Peer Review of the Biomedical Literature*. doi:10.3410/f.733483547.793552311

[13] DiBartola, S. P. (2011, June 22). Applied Renal Physiology. Retrieved February 18, 2019, from https://www.sciencedirect.com/science/article/pii/B9781437706543000093

[14] Drumond, M. C., Kristal, B., Myers, B. D., & Deen, W. M. (1994). Structural basis for reduced glomerular filtration capacity in nephrotic humans. *Journal of Clinical Investigation,94*(3), 1187-1195. doi:10.1172/jci117435

[15] Narsilio, G. A., Buzzi, O., Fityus, S., Yun, T. S., & Smith, D. W. (2009). Upscaling of Navier–Stokes equations in porous media: Theoretical, numerical and experimental approach. *Computers and Geotechnics,36*(7), 1200-1206. doi:10.1016/j.compgeo.2009.05.006

[16] *Advances in separation processes*. (1990). Rugby (Gran Bretaña): Institution of Chemical Engineers.

[17] Kumar, A., Pramanik, S., & Mishra, M. (2016, October). *COMSOL Multiphysics® Modeling in Darcian and Non-Darcian Porous Media.* In Proceedings of the 2016 COMSOL Conference, Bangalore, India (pp. 20-21).

[18] Gerich, J. E. (2010, February). Role of the kidney in normal glucose homeostasis and in the hyperglycaemia of diabetes mellitus: Therapeutic implications. Retrieved from https://www.ncbi.nlm.nih.gov/pmc/articles/PMC4232006/

[19] Kreft, M., Lukšič, M., Zorec, T. M., Prebil, M., & Zorec, R. (2013, April). tgm

[20] Hosten, A. O. (1990, January 01). BUN and Creatinine. Retrieved from https://www.ncbi.nlm.nih.gov/books/NBK305/

[21] Colton, C. K., Smith, K. A., Merrill, E. R., & Friedman, S. (2004, June 17). Diffusion of urea in flowing blood. Retrieved from https://onlinelibrary.wiley.com/doi/pdf/10.1002/aic.690170408

[22] Wakeham, W., Salpadoru, N., & Caro, C. (1976). Diffusion coefficients for protein molecules in blood serum. *Atherosclerosis,25*(2-3), 225-235. doi:10.1016/0021-9150(76)90029-0

[23] Wang, R. E., Tian, L., & Chang, Y. (2012, April 07). A homogeneous fluorescent sensor for human serum albumin. Retrieved from https://www.ncbi.nlm.nih.gov/pmc/articles/PMC3299827/

[24] Kaufman DP, Knohl SJ. (2018 Oct 27). Physiology, Glomerular Filtration Rate (GFR). Retrieved from: https://www.ncbi.nlm.nih.gov/books/NBK500032/